

# Supporting Information

**Title:** Modeling Reactive Transport of Polydisperse Nanoparticles: Assessment of the Representative Particle Approach

**Authors:** Amir Taghavy<sup>1</sup>, and Linda M. Abriola<sup>2,\*</sup>

<sup>1</sup> Department of Civil and Environmental Engineering, University of Massachusetts Dartmouth, MA, 02747

<sup>2</sup> Department of Civil and Environmental Engineering, Tufts University, Medford, MA 02155

# Appendix A – RPA-Error in Approximation of nAg Specific Surface Area

Starting from the basic definitions of converting number-based fractions ( $f_i^N$ ) to mass (or volume – for constant density particles) fractions ( $f_i^m$ ), we can write:

$$f_i^m = \frac{f_i^N \cdot d_{p_i}^3}{\sum_i f_i^N \cdot d_{p_i}^3} \quad (\text{A1})$$

where  $d_{p_i}$  [L] is the diameter of particles in bin  $i$ . The mass-based or volumetric mean diameter ( $d_{50}^m$ ) of a population of variably sized particles can be calculated as:

$$d_{50}^m = \frac{\sum_i f_i^m \cdot d_{p_i}}{\sum_i f_i^m} = \sum_i f_i^m \cdot d_{p_i} \quad (\text{A2})$$

given that  $\sum_i f_i^m = 1$ .

Now and concerning the dissolution kinetics, we assume the rate of  $\text{Ag}^+$  mass speciation from a silver nanoparticle to be proportional to the surface area of that particle [1]. For a population of particles one can assume that dissolution kinetics is proportional to the specific surface area ( $SSA$ ) of particles for any given point in time,  $t$ , and space,  $x$ . That is:

$$\frac{k_{diss}(x,t)}{SSA(x,t)} = \text{constant} \quad (\text{A3})$$

The  $SSA$  of a variably sized population of particles can be calculated directly from the number-based particle size distribution (PSD) as:

$$SSA = \frac{SA}{Vol} = \frac{\sum_i f_i^N \cdot \pi \cdot d_{p_i}^2}{\sum_i f_i^N \cdot \frac{\pi}{6} \cdot d_{p_i}^3} = 6 \cdot \frac{\sum_i f_i^N \cdot d_{p_i}^2}{\sum_i f_i^N \cdot d_{p_i}^3} \quad (\text{A4})$$

where  $SA$  [ $\text{L}^2$ ] and  $Vol$  [ $\text{L}^3$ ] are the total surface area and volume of a population of particles. The rightmost term in Eq. A4 can be rewritten as:

$$SSA = 6 \cdot \frac{\sum_i f_i^N \cdot d_{p_i}^3 / d_{p_i}}{\sum_i f_i^N \cdot d_{p_i}^3} = 6 \cdot \sum_i \frac{1}{d_{p_i}} \cdot \frac{f_i^N \cdot d_{p_i}^3}{\sum_i f_i^N \cdot d_{p_i}^3} \quad (\text{A5})$$

substituting  $f_i^m$  from Eq. A1 in Eq. A5, an expression for calculating  $SSA$  from mass fractions can be derived as:

$$SSA = 6 \cdot \sum_i \frac{f_i^m}{d_{p_i}} \quad (A6)$$

Alternatively,  $SSA$  can be estimated using the mean particle diameter as the diameter of a particle representative of the entire population (i.e. RPA approach). Based on this approach:

$$SSA_{d_{50}^m} = \frac{6}{d_{50}^m} = \frac{6}{\sum_i f_i^m \cdot d_{p_i}} \quad (A7)$$

Given the difference in the mathematical form of  $SSA$  expressions between equations A6 and A7, it can be shown that  $SSA_{d_{50}^m}$  (Eq. A7) is a biased estimator that tends to underestimate  $SSA$  parameter.

# Appendix B – Component Reactive Transport Equations

The numerical model presented in Taghavy et al. [2] is incorporated in this study. Three advection-dispersion-reaction (ADR) equations are solved for represent transport and oxidative dissolution of particulate silver (nAg), where dissolved silver ( $\text{Ag}^+$ ) is speciated, and dissolved oxygen (DO) is consumed [2]:

$$\frac{\partial}{\partial t}(\phi C_i + \rho_b S_i) + \frac{\partial}{\partial x} \left[ \phi \left( v_w C_i - D_{w,i}^h \frac{\partial C_i}{\partial x} \right) \right] = r_i \quad (\text{B1})$$

here subscript  $i$  denotes particulate and dissolved components (i.e. nAg, DO and  $\text{Ag}^+$ ),  $C_i$  (mol/m<sup>3</sup>) is the molar concentration of component  $i$  in the aqueous phase, and  $S_i$  [mol/kg dry sand] is the molar concentration of component  $i$  associated with the sand grains per unit weight of the solid phase,  $\rho_b$  (kg/m<sup>3</sup>) and  $\phi$  [–] are dry bulk density and clean bed porosity of sand,  $v_w$  (m/s) is the interstitial velocity of water, and  $D_{w,i}^h$  (m<sup>2</sup>/s) is hydrodynamic dispersion coefficient of component  $i$  in the aqueous phase. The reaction term  $r^i$  (mol/m<sup>3</sup>.s) is the net molar rate of production of component  $i$  in the aqueous phase per unit bulk volume. nAg dissolution is represented using a first-order kinetic expression with respect to nAg concentration [1] and the stoichiometric coefficients;  $a_{\text{Ag}^+/\text{nAg}} = 1$  and  $a_{\text{DO}/\text{nAg}} = 0.25$ :

$$r^{\text{nAg}} = \frac{\partial}{\partial t}(\phi C_{\text{nAg}} + \rho_b S_{\text{nAg}}) = -k_{\text{diss}}(\theta_w C_w^{\text{nAg}} + \rho_b^* \omega_s^{\text{nAg}}) = -r^{\text{Ag}^+} = 0.25 r^{\text{DO}} \quad (\text{B2})$$

where  $k_{\text{diss}}$  [s<sup>-1</sup>] is the nAg dissolution rate coefficient, a function of the specific surface area (SSA) [m<sup>2</sup>/g]

$$k_{\text{diss}}(x,t) = k_{\text{diss}0} \cdot \frac{\text{SSA}(x,t)}{\text{SSA}_0} \quad (\text{B3})$$

of particles calculated based on the scaling of a reference state denoted with subscript 0:

**Particle-Collector Interactions:** the second term on the time derivative of Eq. B1 accounts for mass transfer between aqueous and solid phases and represents the filtration of nAg.  $\text{Ag}^+$  and DO adsorption to solid phase was neglected.

$$\rho_b \frac{\partial S}{\partial t} = \phi k_{\text{att}} \psi C \quad (\text{B4})$$

where  $\psi$  [–] is a site blocking function assuming a value of unity in the case of clean bed filtration [3], and  $k_{\text{att}}$  (1/s) is particle attachment rate constant and is expressed as a function of the physical and chemical characteristics of particle, flow and porous medium:

$$k_{att} = \frac{3(1-\phi)v_w}{2d_c} \alpha_{PC} \cdot \eta_0 \quad (B5)$$

here  $d_c$  (m) is the mean sand grain diameter, and  $\alpha_{PC}$  and  $\eta_0$  are dimensionless variables denoting the adhesive fraction and frequency of particle-collector collisions. The former parameter is obtained by fitting experimental breakthrough and/or retention data and the latter was calculated a priori using semi-empirical correlation of Tufenkji and Elimelech [4]:

$$\eta_0 = 2.4A_s^{1/3}N_R^{-0.081}N_{Pe}^{-0.715}N_{vdW}^{0.052} + 0.55A_sN_R^{1.675}N_A^{0.125} + 0.22N_R^{-0.24}N_G^{1.11} \quad (B6)$$

where  $A_s$ ,  $N_R$ ,  $N_{Pe}$ ,  $N_{vdW}$ ,  $N_A$ , and  $N_G$  are dimensionless numbers fully described in [4]. Note that with the exception of Happel correction factor,  $A_s$ , and van der Waals number,  $N_{vdW}$ , the remaining dimensionless numbers are particle size-dependent parameters.

# Appendix C – Selected Simulation Results for the Modeled Case Scenarios

Tabulated silver recovery values in terms of particulate (nAg), dissolved (Ag<sup>+</sup>), and total silver elution are presented in Table A2. Values are provided in absolute [mg] and normalized (to injected silver mass of 0.234 mg) [%] forms. Table A3 provides a summary of calculated RPA-error in approximation of silver elution in form of particulate nAg, dissolved Ag<sup>+</sup> ions. Table A4 presents the predicted change in mean particle diameters between influent and effluent boundaries.

*Table A2. Simulated silver recovery from the sand column based on the RPA (MD: monodisperse) approximation and PSD approach that treats NPs as polydisperse (PD) populations for the base case, increased filter length, and reduced flow case scenarios.*

			RPA (MD)			PD #1			PD #2			PD #3		
			nAg	Ag <sup>+</sup>	Tot Ag	nAg	Ag <sup>+</sup>	Tot Ag	nAg	Ag <sup>+</sup>	Tot Ag	nAg	Ag <sup>+</sup>	Tot Ag
Ag mass eluted	Base case	mg	0.144	0.006	0.150	0.139	0.007	0.146	0.120	0.014	0.135	0.110	0.014	0.124
		%	61.5%	2.6%	64.1%	59.6%	3.0%	62.6%	51.3%	6.2%	57.5%	47.0%	6.1%	53.1%
	Increased length	mg	0.087	0.010	0.096	0.083	0.011	0.094	0.070	0.018	0.088	0.059	0.019	0.078
		%	37.0%	4.1%	41.1%	35.4%	4.6%	40.0%	29.9%	7.9%	37.8%	25.0%	8.2%	33.2%
	Reduced velocity	mg	0.015	0.080	0.095	0.015	0.086	0.101	0.017	0.111	0.127	0.015	0.125	0.140
		%	6.3%	34.3%	40.6%	6.6%	36.8%	43.4%	7.2%	47.3%	54.5%	6.4%	53.4%	59.8%

*Table A3. RPA error in the particulate, dissolved, and total silver mass recovery for the base case, increased filter length, and reduced flow case scenarios.*

PSD	Base case			Increased Length			Reduced Velocity		
	nAg	Ag <sup>+</sup>	Total Ag	nAg	Ag <sup>+</sup>	Total Ag	nAg	Ag <sup>+</sup>	Total Ag
PSD #1	3.2%	-13.5%	2.4%	4.5%	-10.7%	2.7%	-3.5%	-6.8%	-6.3%
PSD #2	19.7%	-58.1%	11.3%	23.8%	-47.6%	8.9%	-12.4%	-27.5%	-25.5%
PSD #3	30.7%	-57.4%	20.6%	47.9%	-49.4%	23.9%	-1.6%	-35.8%	-32.1%

Table A4. Mean diameters of effluent particles and respective percent increase from the influent mean particle diameter of ca. 39 nm predicted for PSD#1-3 for the base case, increased filter length, and reduced flow case scenarios.

		PD #1	PD #2	PD #3
Base case	nm	40.2	49.1	54.4
	% increase	4.4%	27.3%	41.0%
Increased length	nm	41.9	57.4	72.7
	% increase	8.7%	48.6%	88.6%
Reduced velocity	nm	47.0	77.0	121.0
	% increase	22.0%	99.5%	213.6%

# Appendix D – Log-Normal Fit to Experimental Particle Size Distribution

The cumulative form of experimental particle size distribution of Zhang et al. [5] was constructed and was fitted to a log-normal distribution (Equation D1).

$$F(d_p, \mu_{LN}, \sigma_{LN}) = \frac{1}{2} + \frac{1}{2} \cdot \operatorname{erf}\left(\frac{\ln(d_p) - \mu_{LN}}{\sqrt{2} \sigma_{LN}}\right) \quad (\text{D1})$$

where  $d_p$ [m] is the independent random variable representing particle diameter, and  $\mu_{LN}$  and  $\sigma_{LN}$  are the lognormal distribution parameters with fitted values of 3.58 and 0.36, respectively.

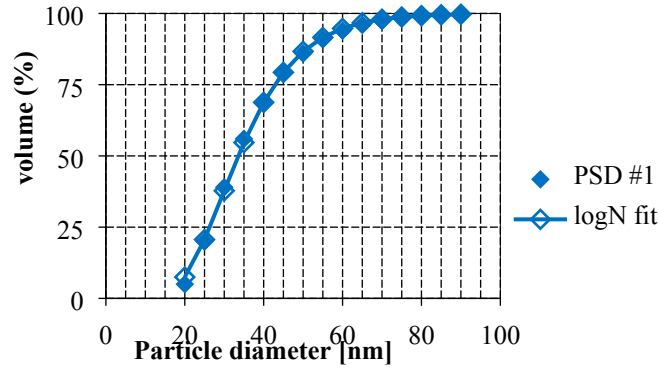


Figure A2. Log-normal fit to the experimental nAg particle-size-distribution.

Parametric estimators of the mean,  $\mu_{d_p}$ , and skewness,  $\gamma_{d_p}$ , for a lognormal distribution are given as:

$$\mu_{d_p} = \exp\left(\mu_{LN} + \frac{\sigma_{LN}^2}{2}\right) \quad (\text{D2.a})$$

$$\sigma_{d_p} = \exp\left(\mu_{LN} + \frac{\sigma_{LN}^2}{2}\right) \sqrt{e^{\sigma_{LN}^2} - 1} \quad (\text{D2.b})$$

$$\gamma_{d_p} = \left(e^{\sigma_{LN}^2} + 2\right) \sqrt{e^{\sigma_{LN}^2} - 1} \quad (\text{D2.c})$$



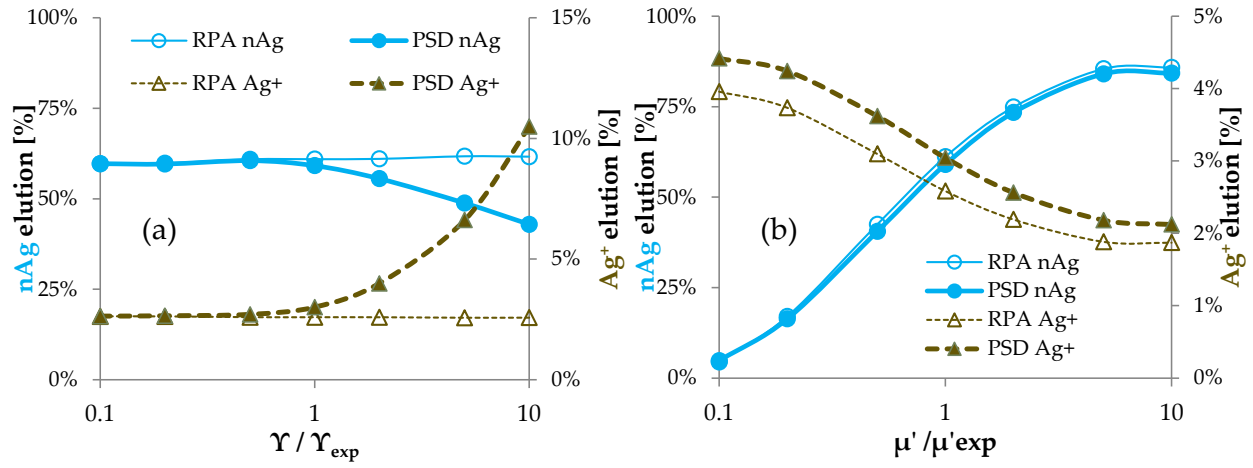


Figure A3. Sensitivity of predicted silver elution in particulate (left vertical axis) and dissolved (right vertical axis) forms as percentage of injected total silver mass ( $234\mu\text{g}$  in all simulations) to variations in (a) distribution skewness at constant mean particle diameter (39 nm) and (b) distribution mean at constant coefficient of variation of 0.37. Note the expected insensitivity of RPA predictions to variations in distribution skewness, a result of the constant mean.

# References

- 1 Liu, J. and Hurt, R. H. Ion release kinetics and particle persistence in aqueous nano-silver colloids. *Environmental science & technology*, 44, 6 (2010), 2169-2175.
- 2 Taghavy, A., Mittelman, A., Wang, Y., Pennell, K. D., and Abriola, L. M. Mathematical modeling of the transport and dissolution of citrate-stabilized silver nanoparticles in porous media. *Environmental science & technology*, 47, 15 (2013), 8499-8507.
- 3 Yao, K. M., Habibian, M. T., and O'Melia, C. R. Water and waste water filtration. Concepts and applications. *Environmental science & technology*, 5, 11 (1971), 1105-1112.
- 4 Tufenkji, N. and Elimelech, M. Correlation equation for predicting single-collector efficiency in physicochemical filtration in saturated porous media. *Environmental Science & Technology*, 38, 2 (2004), 529-536.
- 5 Zhang, W., Yao, Y., Sullivan, N., and Chen, Y. Modeling the primary size effects of citrate-coated silver nanoparticles on their ion release kinetics. *Environmental science & technology*, 45, 10 (2011), 4422-4428.